

Loss of Clusterin shifts amyloid deposition to the cerebrovasculature via disruption of perivascular drainage pathways

Aleksandra Wojtas¹, Silvia Kang¹, Benjamin Olley², Maureen Gatherer², Mitsuru Shinohara³, Patricia Lozano¹, Chia-Chen Liu³, Aishe Kurti¹, Kelsey Baker¹, Dennis Dickson¹, Mei Yue¹, Leonard Petrucelli¹, Guojun Bu³, Roxana Carare², John D Fryer¹

¹Mayo Clinic, ²University of Southampton, ³Mayo Clinic Jacksonville

Submitted to Proceedings of the National Academy of Sciences of the United States of America

Alzheimer's disease (AD) is characterized by amyloid- β (A β) peptide deposition in brain parenchyma as plaques and in cerebral blood vessels as cerebral amyloid angiopathy (CAA). CAA deposition leads to several clinical complications, including intracerebral hemorrhage. The underlying molecular mechanisms that regulate plaque and CAA deposition in the vast majority of sporadic AD patients remain unclear. The clusterin (CLU) gene is genetically associated with AD and CLU has been shown to alter aggregation, toxicity and blood-brain barrier transport of A β , suggesting it might play a key role in regulating the balance between A β deposition and clearance in both brain and blood vessels. Here, we investigated the effect of CLU on A β pathology using the APP/PS1 mouse model of AD amyloidosis on a *Clu*^{+/+} or *Clu*^{-/-} background. We found a marked decrease in plaque deposition in the brain parenchyma but an equally striking increase in CAA within the cerebrovasculature of APP/PS1; *Clu*^{-/-} mice. Surprisingly, despite the several-fold increase in CAA levels, APP/PS1; *Clu*^{-/-} mice had significantly less hemorrhage and inflammation. Mice lacking CLU had impaired clearance of A β *in vivo* and exogenously added CLU significantly prevented A β binding to isolated vessels *ex vivo*. These findings suggest that in the absence of CLU, A β clearance shifts to perivascular drainage pathways resulting in fewer parenchymal plaques but more CAA due to loss of CLU chaperone activity, complicating the potential therapeutic targeting of CLU for AD.

Clusterin | Alzheimer's disease | Cerebral Amyloid Angiopathy | A β | hemorrhage

Introduction

Alzheimer's disease (AD) is the most common form of age-related dementia and represents a major health problem in the growing population of elderly people in developed countries (1). AD is characterized by pathological accumulation of tau as neurofibrillary tangles and deposition of toxic aggregates of amyloid- β (A β) peptide as fibrillar and diffuse plaques, resulting from the proteolytic cleavage of amyloid precursor protein (APP) by β - and γ -secretases (2-6). Additionally, A β can accumulate within the cerebral blood vessel walls, termed cerebral amyloid angiopathy (CAA). CAA is observed in the vast majority of AD patients (7-9), with A β deposition typically occurring in leptomeningeal vessels and penetrating arterioles (10). Several clinical complications arise from CAA, among which intracerebral hemorrhage is the most devastating (11). Additionally, familial forms of CAA arise from mutations within the A β coding region resulting in enhanced A β aggregation in the basement membrane of the cerebrovasculature (12-15).

Rare forms of AD also exist from mutations in amyloid precursor protein (APP) (16, 17) and other causative genes (18-20) leading to accelerated A β production and deposition, predominantly in the form of A β ₄₂ (21, 22). However, it is still unclear what drives A β deposition in the more common sporadic form of

AD. Growing evidence suggests that disruption of A β clearance mechanisms from the brain contributes to its accumulation, ultimately initiating the pathogenic cascade in AD (23). It has been shown that CAA can be induced by the failure of the perivascular drainage pathway to clear A β from the brain along cerebrovascular basement membranes (24). We have discovered several factors involved in perivascular drainage of A β including apolipoprotein E (ApoE), aging, and high fat diet (25-27). Therefore, uncovering additional factors that contribute to A β clearance by any means is critical to further our understanding of how A β plaque and CAA levels are regulated.

Clusterin (CLU), also known as apolipoprotein J (apoJ), is a multifaceted protein that regulates a broad range of biological processes, including lipid metabolism (28-30), apoptosis (31), spermatogenesis (32), and aggregation and adhesion of cells (33). The single CLU gene, located on chromosome 8 in humans (34, 35), encodes a 70-80kDa highly glycosylated protein that is cleaved to form α - and β subunits linked together by disulfide bonds during maturation (36, 37). With a central role in scavenging and survival (38, 39), the secreted form of CLU is a prominent chaperone in extracellular compartments (37). However, it has previously been reported that nuclear forms of CLU also exist from alternative splicing omitting exon 2 or translation from an alternative ATG start codon, although this is unique to the hu-

Significance

Deposition of amyloid- β (A β) peptide in the form of parenchymal plaques and A β accumulation in the walls of cerebral vessels as cerebral amyloid angiopathy (CAA) are pathological hallmarks of Alzheimer's disease (AD). The clusterin (CLU) gene, which confers AD risk, is associated with amyloid deposition. Here we show that loss of CLU promotes cerebrovascular CAA, yet significantly reduces the amount of parenchymal plaques by altering perivascular drainage of amyloid- β in the APP/PS1 mouse model of AD. The absence of CLU in these mice is associated with a lower number of hemorrhage and a decrease in inflammation. These results suggest that CLU functions as a major A β chaperone to maintain A β solubility along interstitial fluid drainage pathways and prevent CAA formation.

Reserved for Publication Footnotes

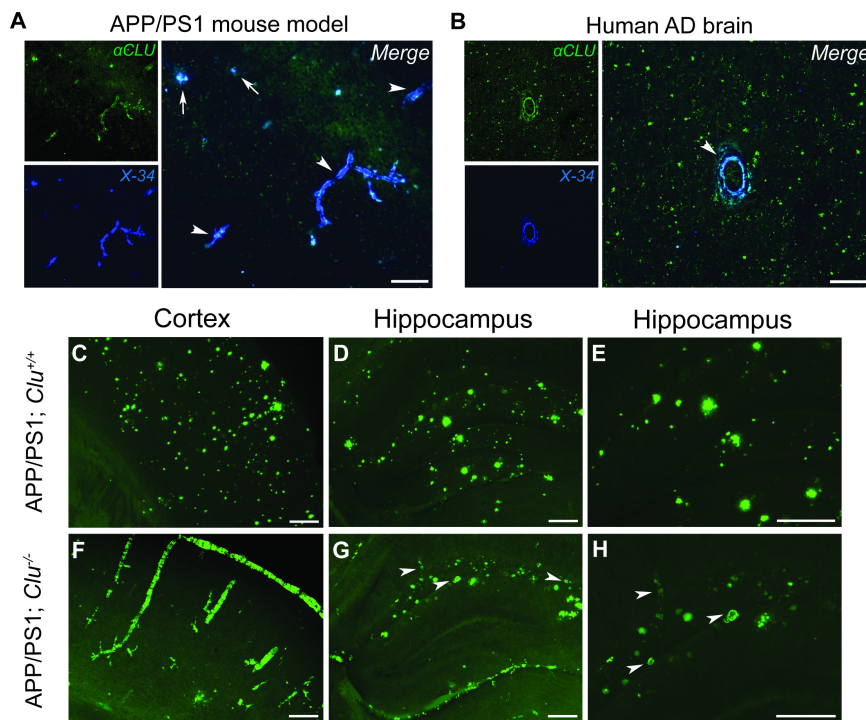


Fig. 1. CLU expression influences A β pathology associated with AD in cortex and hippocampus of 12-month-old APP/PS1 mice. (A-B) CLU-colocalization with amyloid in brain parenchyma and cerebrovasculature in the APP/PS1 mouse model and in human AD brain tissue. X-34 was used to label fibrillar amyloid. Scale bar, 50 μ m. (A) Representative brain section from APP/PS1 mouse showing halo-like co-localization of CLU (green) with amyloid plaques (blue) and complete co-localization with CAA (blue). (B) Representative brain section from patient with CAA showing co-localization of CLU with amyloid in cerebral vessel. Arrows indicate amyloid plaques and arrowheads indicate CAA. (C-E) APP/PS1; *Clu*^{+/+} mice had abundant amyloid plaque pathology by 12 months of age in the cortex and hippocampus. (F-H) However, APP/PS1; *Clu*^{-/-} mice had a striking reduction in the amount of amyloid plaques in brain parenchyma and an increase in the amount of CAA in the cortex and hippocampus. (G-H) Arrowheads indicate A β deposits in small vessels in the hippocampus of APP/PS1; *Clu*^{-/-}, rarely present in APP/PS1; *Clu*^{+/+} mice. (C-H) Thioflavine-S was used to label fibrillary amyloid. Scale bar, 100 μ m.

man transcript. Notably, nuclear CLU has been shown to trigger apoptosis in the cells under pathological conditions (40, 41).

CLU is ubiquitously expressed in most mammalian tissues (29, 42-44), with the highest expression level in the central nervous system (CNS) (45-47). For over two decades the ϵ 4 allele of *APOE* has been recognized as a major risk factor for both AD and CAA development (48, 49). However the role of CLU, another abundantly expressed apolipoprotein in the brain (50), in A β pathology has received significantly less attention. Importantly the levels of CLU have been found to be significantly elevated in AD patients compared to non-demented elderly individuals (51). Moreover, *in vitro* studies have shown that CLU directly interacts with A β (52) and facilitates the formation of toxic A β fibrils (53, 54). Such a role of CLU in amyloid plaque formation, the effect of CLU on A β metabolism and deposition in cerebral vessels was not examined (56). Here, we utilized the well-characterized APP/PS1 mouse model of AD amyloidosis crossed to *Clu* knockout (*Clu*^{-/-}) mice on a pure C57BL/6J background and conducted comprehensive histological and biochemical analyses.

In addition to functional studies supporting the role of CLU in AD, genome wide association studies (GWAS) (60-63) have previously shown that genetic allelic variance in *CLU* single nucleotide polymorphisms (SNPs) are significantly associated with AD risk. More recently, rare *CLU* variants associated with AD have also been identified (64). Although a previous study utilizing a transgenic mouse model of AD (PDAPP model) investigated the role of CLU in amyloid plaque formation, the effect of CLU on A β metabolism and deposition in cerebral vessels was not examined (56). Here, we utilized the well-characterized APP/PS1 mouse model of AD amyloidosis crossed to *Clu* knockout (*Clu*^{-/-}) mice on a pure C57BL/6J background and conducted comprehensive histological and biochemical analyses.

Our findings have demonstrated that loss of CLU led to abundant CAA but simultaneously reduced brain parenchymal amyloid deposits. Despite the dramatic increase in CAA, the APP/PS1; *Clu*^{-/-} mice presented with a significantly lower number of spontaneous hemorrhages and an overall decrease in inflammation and neuritic dystrophy compared to APP/PS1; *Clu*^{+/+} littermates. Importantly, we have provided *in vivo* evidence that

loss of CLU is sufficient to alter the efficiency of the A β clearance from the brain. Finally, the presence of exogenous CLU decreased the amount of A β ₄₀ and A β ₄₂ associated with cerebrovasculature in *ex vivo* binding experiments, suggesting that in the absence of CLU the clearance of A β shifts to more perivascular drainage but results in the deposition of amyloid in the vessel walls as CAA due to loss of CLU chaperone function. Together, this study suggests a novel role for CLU in mediating perivascular clearance of A β from the brain but also indicates that therapeutic targeting of CLU might unintentionally shift pathology to CAA.

Results

CLU co-localizes with plaques and CAA and CLU expression determines amyloid distribution during pathological accumulation of A β

To examine the impact of CLU on amyloid pathology, we first investigated the pattern of CLU co-localization with A β deposits in brain parenchyma and cerebrovasculature in APP/PS1 transgenic mice (65). In this mouse model there is rapid A β accumulation in the brain and development of CAA-associated hemorrhage (66). CLU immunostaining with the Congo red derivative X-34 counterstaining to label fibrillar amyloid revealed intense labeling of CLU with a "halo-like" appearance surrounding amyloid plaques in the brain parenchyma (Fig. 1A). CLU also extensively co-localized to A β deposits in cerebral blood vessels in APP/PS1 mice (Fig. 1B). In addition, CLU showed association with A β deposits in human cortex from an AD case with complete co-localization with CAA (Fig. 1B).

We then set out to determine whether changes in CLU levels influenced A β accumulation in the brain. We bred APP/PS1 mice onto a *Clu*^{+/+} or a *Clu*^{-/-} background (littermates on C57BL/6J background strain) and harvested PBS perfused brains at 6 and 12 months of age. Immunohistochemical analysis of A β and thioflavine-S staining revealed that CLU loss did not impact the onset of A β deposition in the brain but substantially influenced where A β accumulated. Specifically, 6- and 12-month-old APP/PS1; *Clu*^{+/+} mice showed A β deposition mostly in the form

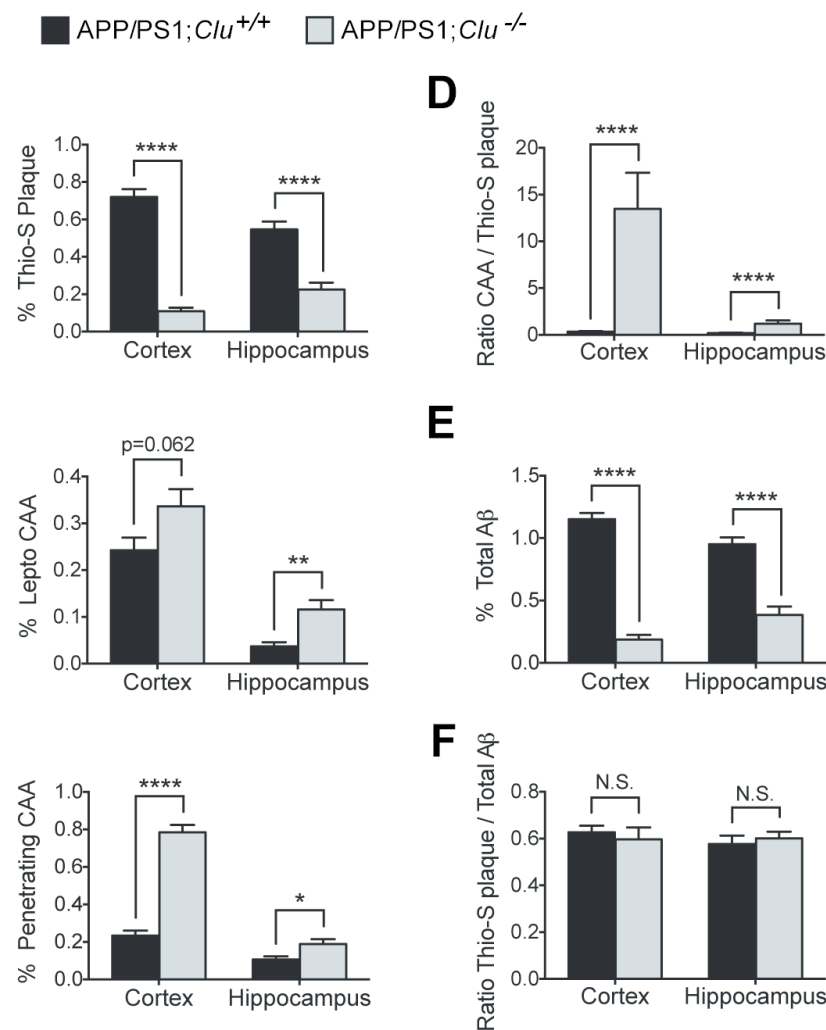


Fig. 2. Stereological quantification of amyloid deposition in brain parenchyma and cerebrovasculature in 12-month-old APP/PS1 mice. (A) 12-month-old APP/PS1; *Clu*^{-/-} mice had a significant decrease in the amount of amyloid plaques in cortex and hippocampus. (B) Significant increase in amyloid in leptomeningeal vessels and (C) penetrating arterioles was observed in the absence of CLU in cortex and hippocampus. (D) The ratio of CAA to thio-S positive plaques was significantly increased in 12-month-old APP/PS1; *Clu*^{-/-} mice. (E) 12-month-old APP/PS1; *Clu*^{-/-} mice also showed a decrease in the amount of total Aβ in the brain parenchyma in cortex and hippocampus. (F) The ratio of thio-S positive amyloid plaques to total Aβ was not different between CLU genotypes in cortex and hippocampus. Thioflavine-S (thio-S) was used to visualize fibrillar amyloid. N=11-13 mice/group. For each animal three brain sections were analyzed. Data are presented as mean ± s.e.m. and analyzed by Mann-Whitney test; *P<0.05, **P<0.01, ****P<0.0001, N.S. not significant.

of parenchymal plaques observed in the cortex (Fig. S1A and Fig. 1C) and hippocampus (Fig. S1B-S1C and Fig. 1D-1E) whereas in APP/PS1; *Clu*^{-/-} mice, Aβ was predominantly deposited in the cerebrovasculature as CAA (Fig. S1D-1F and Fig. 1F-1H). To more thoroughly analyze this dramatic shift in Aβ localization, we performed an unbiased stereological quantification of thioflavine-S positive deposits in brain parenchyma and cerebrovasculature in 6- and 12-month-old mice (Fig. S2 and Fig. 2). We observed a highly significant reduction in the amount of thioflavine-S positive plaques in 6-month-old APP/PS1; *Clu*^{-/-} mice in cortex (P<0.0001; Fig. S2A) and hippocampus (P<0.05; Fig. S2A) compared to control APP/PS1; *Clu*^{+/+} littermates. The absence of CLU also caused an increase in thioflavine-S positive Aβ accumulation in leptomeningeal vessels (P<0.01 in cortex and P<0.05 in hippocampus; Fig. S2B) and penetrating arterioles (P<0.05 in cortex and hippocampus; Fig. S2C) at 6 months of age. Similarly, 12-month-old APP/PS1; *Clu*^{-/-} mice also showed reduced thioflavine-S positive deposits in parenchymal plaques (P<0.0001 in cortex and hippocampus; Fig. 2A) and increased CAA in leptomeningeal vessels of cortex (P=0.062; Fig. 2B) and hippocampus (P<0.01; Fig. 2B) and penetrating arterioles (P<0.001 in cortex and P<0.05 in hippocampus; Fig. 2C). In addition, the ratio of CAA to amyloid plaques was significantly increased in these brain regions in 12-month-old APP/PS1; *Clu*^{-/-} mice compared to APP/PS1; *Clu*^{+/+} mice (Fig. 2D). Quantita-

tively, we observed a 40-fold and 6-fold increase in the ratio of CAA to parenchymal amyloid load in cortex (P<0.0001) and hippocampus (P<0.0001) of 12-month-old animals, respectively (Fig. 2D). Similarly, at 6 months of age, the ratio of CAA to amyloid plaques was 50-fold increased in cortex (P<0.0001) and 5-fold increased in hippocampus (P<0.01) (Fig. S2D). Numerous small vessels of the hippocampus were thioflavine-S positive in APP/PS1; *Clu*^{-/-} mice (Fig. S1E-1F and Fig. 1G-1H), a feature rarely seen in this APP/PS1 model.

Given that Aβ peptide accumulates in the brain in the form of fibrillar (thioflavine-S positive) and diffuse (thioflavine-S negative) plaques, we next examined the total amount of Aβ in the same animal cohort by Aβ immunostaining and stereological quantification. We observed a significant decrease in total Aβ plaque levels in 6- (P<0.0001 in cortex and P<0.05 in hippocampus; Fig. S2E) and 12-month-old (P<0.0001; Fig. 2E) APP/PS1; *Clu*^{-/-} mice compared to APP/PS1; *Clu*^{+/+} littermates. Additionally, the ratio of fibrillar plaques to total Aβ did not differ between CLU genotypes (Fig. S2F and 2F) with the exception of the cortical region of 6-month old animals that showed a significant reduction in this ratio in APP/PS1; *Clu*^{-/-} mice in relation to APP/PS1; *Clu*^{+/+} mice (P<0.0001; Fig. S2F). Finally, we evaluated sex-dependent effects of CLU on amyloid pathology in 6- and 12-month old-mice (Fig. S3 and Fig. S4). We observed significant differences in amyloid plaque formation (Fig. S3E, Fig. S4A and S4E) and CAA in penetrating vessels (Fig. S3G,

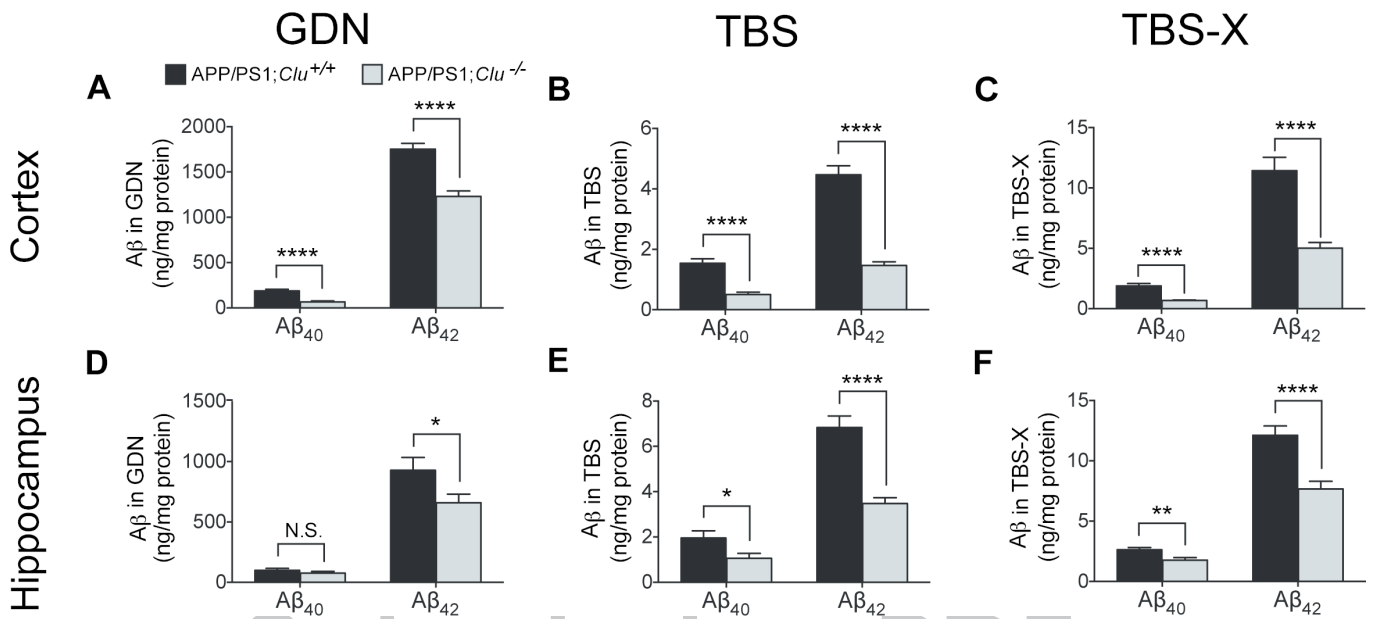


Fig. 3. CLU expression alters the levels of soluble and insoluble Aβ in cortex and hippocampus of 12-month-old APP/PS1 mice. (A-F) Quantification of the Aβ levels in cortex and hippocampus of 12-month old APP/PS1 mice by ELISA. (A) APP/PS1; *Clu*^{+/+} mice showed a significant decrease in the levels of insoluble Aβ₄₀ and Aβ₄₂ in cortex compared to control APP/PS1; *Clu*^{+/+}. (B, C) APP/PS1; *Clu*^{-/-} mice had also reduced levels of (B) soluble and (C) detergent-soluble concentrations of Aβ₄₀ and Aβ₄₂ in cortex. (D) The levels of insoluble Aβ₄₂ but not Aβ₄₀ in hippocampus of APP/PS1; *Clu*^{-/-} mice were also reduced. (E, F) Concentration of (E) soluble and (F) detergent-soluble levels of Aβ₄₀ and Aβ₄₂ in hippocampus were decreased in the absence of CLU. N= 15-23 mice/group. Data are presented as mean ± s.e.m. and analyzed by Mann-Whitney test. *P<0.05, **P<0.01, ****P<0.0001, N.S. not significant.

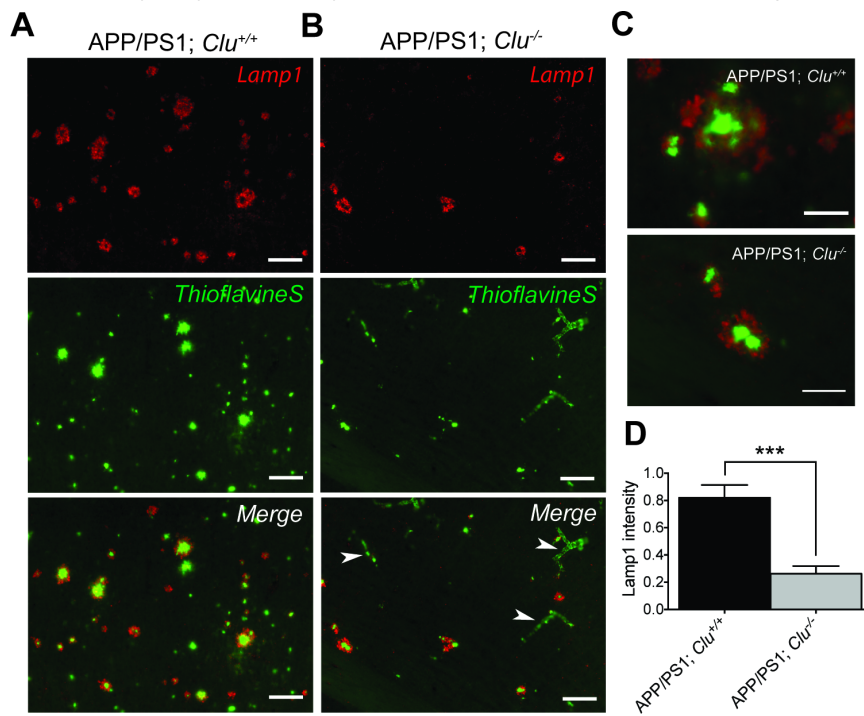


Fig. 4. Absence of CLU reduces the total amount of neuritic dystrophy in APP/PS1 mice. (A) In APP/PS1; *Clu*^{+/+} mice all parenchymal plaques (green) were surrounded by dystrophic neurites (red) identified with Lamp1 antibody. (B) APP/PS1; *Clu*^{-/-} mice had an overall reduction in the amount of parenchymal plaques and a concomitant reduction in total neuritic dystrophy. Arrowheads indicate CAA. (A-B) Scale bar, 50μm. (C) However, prominent neuritic dystrophy was seen around parenchymal plaques that do form in APP/PS1; *Clu*^{-/-} mice. Scale bar, 20μm. (D) Quantification of Lamp1 intensity in brain sections of 12-month-old APP/PS1 mice. N=8-12 mice/group. Data are presented as mean ± s.e.m. and analyzed by Mann-Whitney test. ***P<0.001.

Fig. S4C and S4G) in 6- and 12-month-old animals with females having significantly more Aβ deposition in brain parenchyma and vasculature, suggesting a sex-associated increase in the severity of pathological presentation.

CLU expression alters soluble and insoluble Aβ levels

Since CLU expression significantly impacts where Aβ deposits in the brain, we next examined whether CLU genotype alters the levels of extractable forms of Aβ. Enzyme-linked immunosorbent assay (ELISA) was used to analyze insoluble

(guanidine-HCl fraction, GDN) as well as TBS-soluble and detergent soluble (TBS with Triton-X-100, TBSX) forms of Aβ₄₀ and Aβ₄₂ from cortex and hippocampus of 6- and 12-month-old APP/PS1; *Clu*^{+/+} and APP/PS1; *Clu*^{-/-} mice (Fig. S5 and Fig. 3). In both APP/PS1; *Clu*^{+/+} and APP/PS1; *Clu*^{-/-} mice, substantially higher concentrations of Aβ₄₀ and Aβ₄₂ were found in the insoluble fraction relative to soluble Aβ forms within each genotype (Fig. S5 and Fig. 3), reflecting that the majority of

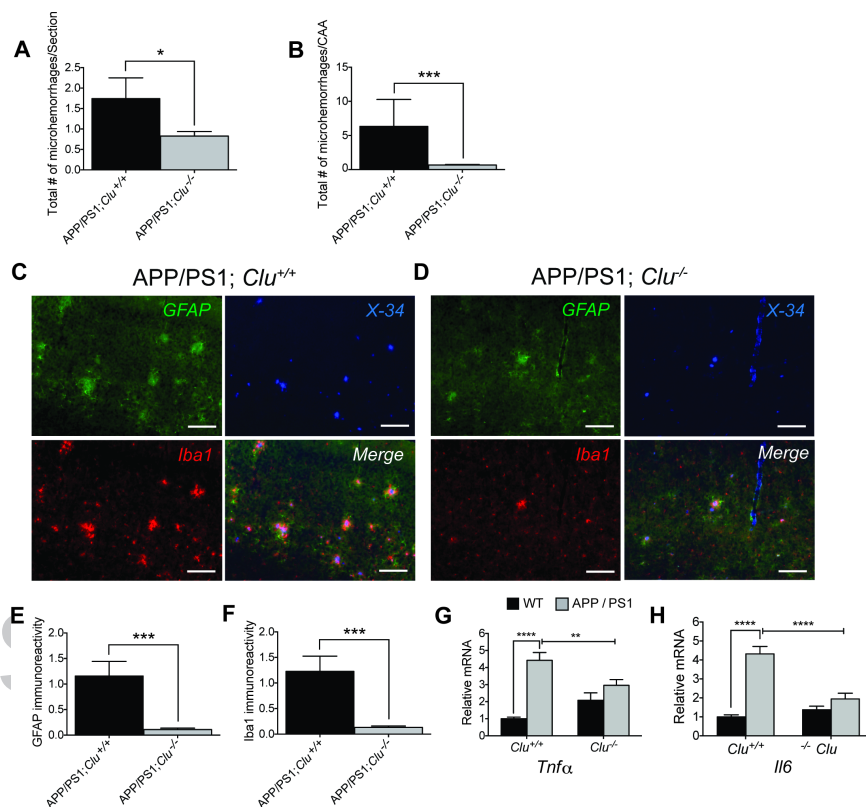


Fig. 5. The absence of CLU in APP/PS1 mice prevents hemorrhage and inflammation at the cellular and molecular level. (A-B) Quantification of CAA-associated hemorrhage in 12-month-old APP/PS1 mice. (A) Despite the abundant increase in CAA, APP/PS1; *Clu*^{-/-} mice had significantly reduced total number of microhemorrhages and (B) number of microhemorrhages normalized to CAA load compared to control APP/PS1; *Clu*^{+/+} animals. (C) APP/PS1; *Clu*^{+/+} mice had abundant astrogliosis (green) and microgliosis (red) surrounding amyloid plaques (blue). (D) Despite the dramatic increase in CAA in APP/PS1; *Clu*^{-/-} mice, the overall level of gliosis was significantly reduced. (C-D) Scale bar, 50μm. (E) Quantification of astrogliosis showed the significant decrease in the number of reactive astrocytes in APP/PS1; *Clu*^{-/-} mice compared to control. (F) Quantification of microgliosis showing reduction of reactive microglia in APP/PS1; *Clu*^{-/-} mice compared to APP/PS1; *Clu*^{+/+} animals. (G-H) APP/PS1; *Clu*^{+/+} mice had increased levels of proinflammatory cytokines such as *Tnfa* and *Il6* compared to non-transgenic (nTg) *Clu*^{+/+} animals. However, this increase in proinflammatory cytokines was significantly reduced in APP/PS1; *Clu*^{-/-} mice. (A-B) N=11-13 mice/group. For each animal 18-21 brain sections were analyzed. Data are presented as mean ± s.e.m. and analyzed by Student's t-test; * P<0.05 and *** P<0.001. (E-F) N=7-11 mice/group. Data are presented as mean ± s.e.m. and analyzed by Student's t-test; ***P<0.001. (G-H) N=8-10 mice/group. Data are presented as mean ± s.e.m. and analyzed by two-way ANOVA with post-hoc Tukey's test. **P<0.01, ****P<0.0001.

Aβ is deposited as insoluble parenchymal plaques and CAA, respectively. Relative to controls, APP/PS1; *Clu*^{-/-} mice showed significantly lower levels of Aβ₄₀ and Aβ₄₂ in the GDN fraction from cortex at 6 and 12 months of age (P<0.0001; Fig. S5A and 3A) and Aβ₄₂ from hippocampus at 6 and 12 months of age (P<0.05; Fig. S5D and 3D). Hippocampal levels of insoluble Aβ₄₀ were not statistically different between CLU genotypes (Fig. S5D and 3D). Similarly, TBS and TBS-X soluble fractions showed dramatic reduction of Aβ₄₀ and Aβ₄₂ levels in the cortex of 6- (P<0.01 and P<0.0001; Fig. S5B and P<0.0001; Fig. S5C) and 12-month old (P<0.0001; Fig. 3B and P<0.0001; 3C) APP/PS1; *Clu*^{-/-} mice in relation to control APP/PS1; *Clu*^{+/+} mice. Additionally, we found that hippocampal concentrations of soluble Aβ₄₀ and Aβ₄₂ of 12-month old mice APP/PS1; *Clu*^{-/-} (P<0.05, P<0.0001; Fig. 3E and P<0.01, P<0.0001; 3F) and Aβ₄₂ of 6-month old mice APP/PS1; *Clu*^{-/-} (P<0.001; Fig. S5E and P<0.01; Fig. S5F) were significantly decreased relative to APP/PS1; *Clu*^{+/+} controls. These data indicate that CLU expression alters the biochemical levels of Aβ deposition and is in agreement with the histological results.

Loss of CLU significantly reduces parenchymal plaque load and neuritic dystrophy

Previous studies utilizing AD mouse models have shown that severely dystrophic neurites surround fibrillar thioflavine-S

positive plaques in the brain parenchyma in a CLU-dependent manner (56). To determine whether CLU genotype affects neuritic dystrophy, we performed double labeling of brain sections with Lamp1, to mark dystrophic neurites, and thioflavine-S, to define fibrillar plaques (Fig. S6A-C and Fig. 4A-C). As expected, we found numerous dystrophic neurites around parenchymal plaques in 6- (Fig. S6A) and 12-month-old APP/PS1; *Clu*^{+/+} mice (Fig. 4A) but none observed in proximity to CAA alone (Fig. S6B and Fig. 4B). APP/PS1; *Clu*^{-/-} mice had a significant reduction in the amount of fibrillar thioflavine-S plaques and a corresponding reduction in the overall amount of neuritic dystrophy compared to APP/PS1; *Clu*^{+/+} mice (Fig. S6B, S6D and Fig. 4B, 4D). However, although CLU has previously been reported to dissociate neuritic dystrophy from fibrillar amyloid plaques (56), we found no evidence of reduced neuritic dystrophy surrounding the few fibrillar thioflavine-S positive plaques that were detected in APP/PS1; *Clu*^{-/-} mice (Fig. S6C and Fig. 4C). The discrepancy between our results and previous reports may be due to differences in the APP transgenic model or the mixed genetic background of Demattos et al., which also raises the possibility that other genetic modifiers are present that mediate the amyloid associated neuritic dystrophy.

Despite increases in CAA, absence of CLU reduces hemorrhage and neuroinflammation associated with Aβ pathology

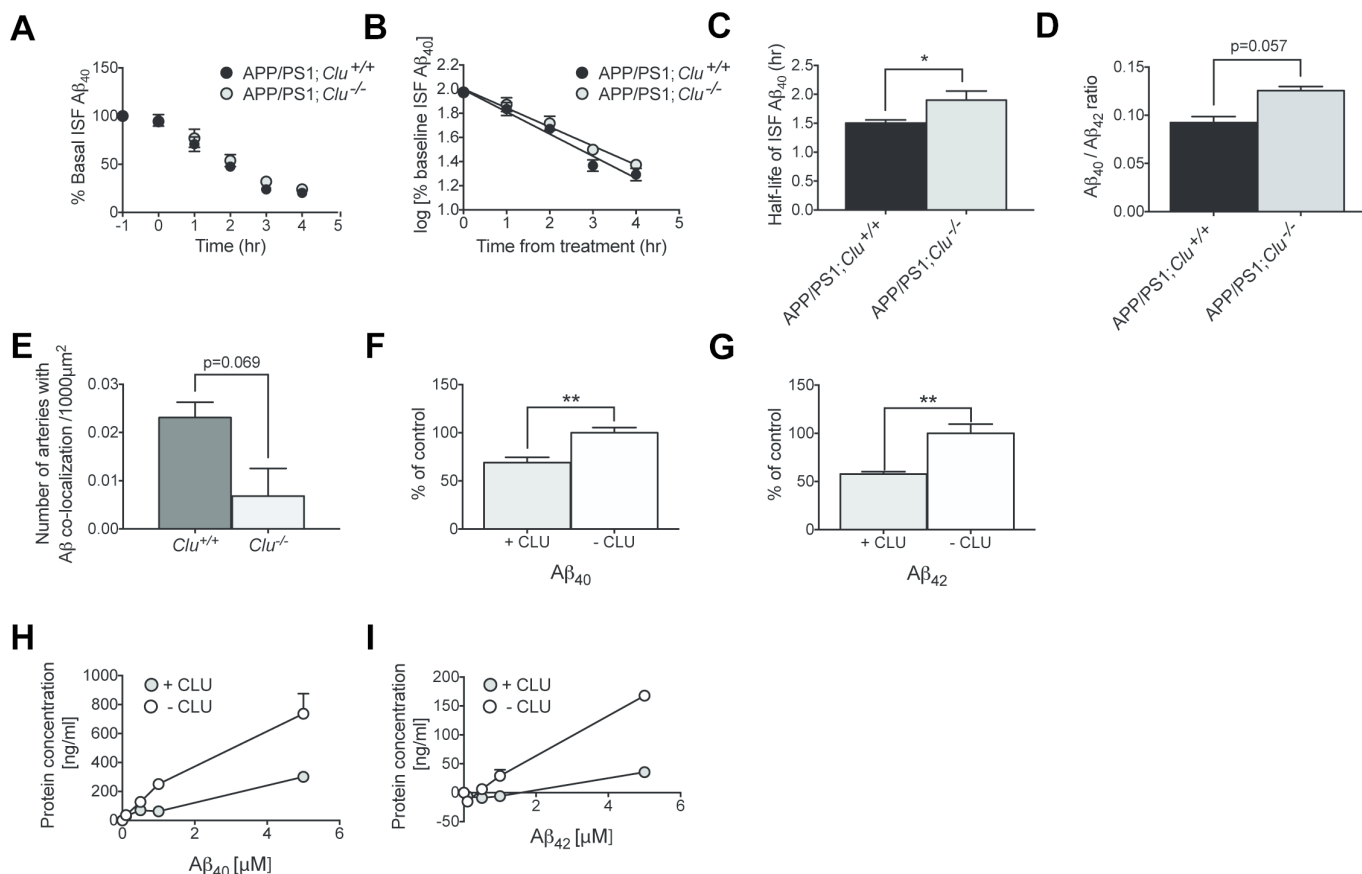


Fig. 6. CLU alters Aβ clearance and prevents binding of soluble Aβ to cerebrovasculature. (A-C) *In vivo* microdialysis to assess the Aβ metabolism in the hippocampus of 10-week-old APP/PS1; *Clu*^{+/+} and APP/PS1; *Clu*^{-/-}. (A) The concentration of Aβ₄₀ in ISF was measured as the basal level of Aβ. (B) The logarithm (log) of percentage baseline ISF Aβ₄₀ versus time was plotted after treatment of mice with a potent γ-secretase inhibitor. (C) The slope from the linear regressions from log (% ISF Aβ₄₀) was used to assess the half-life of Aβ₄₀ elimination from the ISF. (D) The ratio of Aβ₄₀:42 was examined from 10-week-old APP/PS1; *Clu*^{+/+} and APP/PS1; *Clu*^{-/-}. (E) Quantification of the number of arteries with co-localization of fluorescently labeled human Aβ₄₀. Fewer arteries with Aβ co-localization were observed in *Clu*^{-/-} mice compared to *Clu*^{+/+} animals. (F-G) Exogenous (F) Aβ₄₀ and (G) Aβ₄₂ were applied to isolated cerebral vessels with and without exogenously added CLU and binding of Aβ was measured by ELISA. The addition of 1μM exogenous CLU led to a significant reduction in the levels of (F) Aβ₄₀ and (G) Aβ₄₂ associated with cerebrovasculature. (H-I) Isolated vessels were treated with increasing concentrations of exogenous (H) Aβ₄₀ and (I) Aβ₄₂ in the absence and presence of increasing concentrations of CLU. CLU addition resulted in a decrease amount of (H) Aβ₄₀ and (I) Aβ₄₂ bound to cerebral vessels even at high Aβ concentrations. Data presented as ELISA replicates. (A-C) N= 5-6 mice/group. Data are presented as ± s.e.m and analyzed by Student's t-test. *P<0.05. (E-I) N= 3-4 mice/group. Data are presented as ± s.e.m and analyzed by Student's t-test. **P<0.01.

CAA is known to cause cerebral hemorrhage in AD patients (24). To examine if the elevated CAA observed in APP/PS1; *Clu*^{-/-} mice was also associated with increased occurrence of cerebral hemorrhage, Prussian blue staining was conducted on 12-month-old APP/PS1; *Clu*^{+/+} and APP/PS1; *Clu*^{-/-} mice (N≥18 sections/mouse spaced 300μ apart). APP/PS1 mice predominantly develop microhemorrhages in cortex and hippocampus since these two regions are the most severely affected by CAA. Despite the fact that they had substantially increased CAA, we found that APP/PS1; *Clu*^{-/-} mice had significantly fewer spontaneous microhemorrhages compared to control APP/PS1; *Clu*^{+/+} mice (P<0.05; Fig. 5A). When microhemorrhages were normalized to CAA load, we observed an even greater disparity between APP/PS1; *Clu*^{+/+} and APP/PS1; *Clu*^{-/-} mice (P<0.001; Fig. 5B).

Given that both parenchymal plaques and CAA are independently associated with neuroinflammation (67), we next investigated whether CLU genotype had a differential effect on gliosis. Abundant astrogliosis was present around amyloid plaques in brain parenchyma of APP/PS1; *Clu*^{+/+} mice (Fig. 5C). Although the absence of CLU resulted in a dramatic increase in CAA, the level of astrogliosis was significantly reduced when assessed at 12 months of age in APP/PS1; *Clu*^{-/-} mice (Fig. 5D and 5E).

Similarly, APP/PS1; *Clu*^{-/-} mice had significantly decreased microgliosis compared to APP/PS1; *Clu*^{+/+} mice (Fig. 5D and 5F). Reactive astrocytes and microglia were not observed in proximity to CAA regardless of *Clu* genotype (Fig. 5D). To test whether *Clu* genotype also affected neuroinflammation at the molecular level, we profiled inflammatory cytokine transcripts, tumor necrosis factor alpha (*Tnfα*) and interleukin 6 (*Il6*), by real-time quantitative PCR (RT-qPCR). The levels of *Tnfα* and *Il6* were significantly increased in APP/PS1; *Clu*^{+/+} compared to non-transgenic *Clu*^{+/+} littermates but these levels were significantly reduced to near baseline (non-transgenic levels) in APP/PS1; *Clu*^{-/-} mice (Fig. 5G-5H). Taken together, these experiments demonstrate that the majority of inflammation in the presence of amyloid is due to parenchymal plaques rather than CAA, at least in the absence of CLU.

CLU does not impact APP processing or cause widespread transcriptional changes in known Aβ metabolism pathways

The intriguing association between loss of CLU and dramatic increase in CAA led us to determine whether CLU alters APP metabolism. We performed Western blot analysis to assess the level of full length APP and soluble APPα (sAPPα) in brain homogenates of APP/PS1; *Clu*^{+/+} and APP/PS1; *Clu*^{-/-} mice (Fig.

S7A). CLU genotype did not alter APP and sAPP α expression levels indicating that CLU does not grossly affect APP processing (**Fig. S7B** and **S7C**).

A myriad of other factors besides APP processing could explain the shift in A β pathology from parenchymal plaques to CAA. We therefore sought to determine whether specific CLU-dependent changes occurred in the brain transcriptome that might explain this shift in pathology. To identify differentially expressed transcripts between CLU genotypes, we performed an RNAseq transcriptomic study of whole brain tissue from 6-month-old *Clu*^{+/+} and *Clu*^{-/-} mice (n=4/genotype). However, this analysis yielded only four protein coding transcripts that were differentially expressed after false discovery rate correction between *Clu*^{+/+} and *Clu*^{-/-} mice including *Clu* itself, *Slc25a37*, *Hprt*, and *Frem1* (**Table S1**). No significant changes were found in other AD genes such as *Apoe*, *Bin1*, *Abca7*, *Picalm*, *Cd33*, *Cd2ap*, or any of the several putative A β degrading enzymes (**Table S2**). It has previously been shown that overexpression of *Tgfb1* in APP transgenic mice results in a shift in A β pathology from parenchyma to vessels (68), but our transcriptome study did not show any significant changes in *Tgfb1* or the TGF- β pathway in general. These findings suggest that CLU deficiency itself does not significantly impact the whole brain transcriptome and that the effects seen on A β deposition are likely direct in nature.

CLU alters A β clearance pathway and prevents *ex vivo* binding of A β to isolated cerebrovasculature.

To gain insight into the possible mechanism underlying the dramatic shift in the A β deposition from parenchyma to cerebrovasculature in APP/PS1; *Clu*^{-/-} mice, we utilized *in vivo* microdialysis (**Fig. 6A-C**). Since soluble A β in the interstitial fluid (ISF) has been shown to correlate with A β deposited in the brain parenchyma (69) we measured the hippocampal steady state levels in 10-week-old APP/PS1; *Clu*^{+/+} and APP/PS1; *Clu*^{-/-} mice. To determine whether CLU genotype had a differential effect on A β clearance we infused a potent γ -secretase inhibitor that rapidly blocked A β production therefore allowing us to examine the half-life ($t_{1/2}$) of A β_{40} . The concentration of hippocampal A β_{40} , measured in ISF, gradually decreased over time with APP/PS1; *Clu*^{+/+} showing faster decline compared to APP/PS1; *Clu*^{-/-} mice (**Fig. 6B**). Moreover the $t_{1/2}$ of ISF A β_{40} was significantly longer in mice lacking CLU compared to control littermates (**Fig. 6C**). These results suggest that the loss of CLU may alter the clearance of soluble A β from the ISF.

Numerous studies have previously shown that A β_{40} is predominantly present in vascular amyloid due to its more soluble nature (70, 71), whereas A β_{42} , a more fibrillogenic form of A β , is mainly found in parenchymal amyloid (72, 73). Therefore the ratio of A β_{40} :42 seems to determine where A β deposits in the brain with higher A β_{40} :42 ratio predisposing the formation of CAA (74). In agreement with this hypothesis, we found a slight increase in the A β_{40} :42 ratio (p=0.057; **Fig. 6D**) in APP/PS1; *Clu*^{-/-} mice compared to APP/PS1; *Clu*^{+/+} mice.

Given that CAA and AD appear to result from a disruption of perivascular drainage pathway (24, 75), we sought to investigate the potential role of CLU in the A β removal along the basement membrane of cerebral vessels. Therefore, we examined the pattern of distribution of fluorescently labeled human A β_{40} following its intracerebral injection of 3-month old *Clu*^{+/+} and *Clu*^{-/-} mice as we have previously described (25, 26). The difference in counts of arteries with A β co-localization between the injection site and 100 μ m posterior was calculated as a measure of perivascular drainage 10 minutes after injection of fluorescently labeled A β_{40} . We detected fewer arteries with fluorescent A β localization in *Clu*^{-/-} mice compared to control littermates (p=0.069; **Fig. 6E**) suggesting that perivascular drainage of A β might be compromised in the brains of *Clu*^{-/-} animals.

These findings led us to evaluate whether there was a direct effect of CLU on CAA by measuring the ability of CLU to alter binding of A β to the cerebrovasculature in an *ex vivo* binding assay. To this end, we freshly isolated cerebral vessels using density-mediated separation to purify vessels from parenchymal components, as previously described (76). Vessels were then treated with exogenous human A β_{40} or A β_{42} in the presence or absence of exogenous CLU and then washed, lysed in GDN buffer, and A β levels were assessed by ELISA assay. We found that addition of exogenous CLU resulted in a significant reduction of the amount of A β_{40} (P<0.01; **Fig. 6F**) and A β_{42} (P<0.01; **Fig. 6G**) bound to isolated cerebral blood vessels compared to samples lacking exogenous CLU. A similar effect was observed when isolated cerebral vessels were treated with increasing concentrations of exogenous A β_{40} or A β_{42} in the presence of equally increasing concentrations of exogenous CLU (**Fig. 6H** and **6I**). The addition of exogenous CLU led to a dramatic decrease of the level of A β associated with the cerebrovasculature compared to vessels without CLU added, even when assessed at high A β concentrations. Taken together, these results suggest that in the absence of CLU, A β clearance shifts to perivascular drainage resulting in decreased parenchymal amyloid but resulting in the aggregation and deposition in the cerebral blood vessels due to loss of CLU chaperone activity.

Discussion

In the present study, we investigated whether alterations in CLU expression affect amyloid driven pathology. Using the APP/PS1 mouse model of AD amyloidosis, we showed that in sharp contrast to the abundant brain parenchymal amyloid plaque accumulation and minimal CAA observed in APP/PS1; *Clu*^{+/+} mice, APP/PS1; *Clu*^{-/-} mice had few parenchymal plaques but robust CAA, even when assessed at a young age. In addition, CLU loss resulted in substantial alterations of dynamic pools of soluble and insoluble A β . We further demonstrated that lack of CLU significantly reduced the number of CAA-associated microhemorrhages, despite the fact that the APP/PS1; *Clu*^{-/-} mice had a tremendous elevation in the amount of CAA. Our *in vivo* data also showed that APP/PS1; *Clu*^{-/-} mice exhibited significantly less neuritic dystrophy and reduced cellular and molecular inflammation compared to APP/PS1; *Clu*^{+/+} mice. Importantly, by using *in vivo* microdialysis, we provided evidence that CLU is involved in the elimination of A β from the brain. Consistent with this notion, intracerebral injections of A β_{40} of young *Clu*^{+/+} and *Clu*^{-/-} mice resulted in a decreased number of arteries with fluorescently labeled A β_{40} implying the disruption of perivascular drainage pathway in the absence of CLU. Finally, we identified that the presence of exogenously added CLU reduced binding of A β_{40} and A β_{42} to isolated cerebral vessels, suggesting that CLU impacts A β pathology in vessels by preventing it from binding and aggregating during ISF drainage.

Growing evidence suggests that CLU is an important player in A β deposition, fibrillogenesis, and clearance (53, 55-57). The *in vivo* consequences of CLU loss were previously assessed in the PDAPP mouse model of AD (55, 56). These seminal reports showed that absence of CLU was associated with a substantial reduction of fibrillar amyloid plaques but no change in total A β deposition in brain parenchyma. Our data is in agreement with the effect of CLU on fibrillar plaques but, in contrast, we found that loss of CLU also reduced total A β load.

One of the most striking phenotypes of CLU loss in our AD amyloidosis model was the shift in the localization of A β deposition from parenchymal plaques to CAA. Although DeMattos et al. did not directly analyze CAA levels in their study, such an obvious pathology would have been readily noticed. Therefore, the differences in these studies likely reflect the different APP

transgenic models used (PDAPP vs APP/PS1) and/or the mixed genetic background of the PDAPP mouse model.

In light of increasing evidence that disruption of A β clearance mechanisms from the brain initiates the pathogenic cascade of AD (23), identifying factors that contribute to A β elimination is critical. Importantly, we showed that the loss of CLU is sufficient to reduce the efficiency of A β clearance in the hippocampus in our mouse model of AD amyloidosis. In agreement with this observation, we found an increased A β ₄₀:42 ratio in APP/PS1; *Clu*^{-/-} mice, possibly contributing to the shift of A β deposition between brain compartments. Given that A β ₄₀ appears to mediate accumulation of amyloid in cerebral vessels (70, 71), whereas A β ₄₂ is thought to be a predominant form present in the brain parenchyma (72, 73), A β ₄₀:42 ratio might be an important factor in determining where A β deposits.

In fact, several lines of evidence have previously suggested that a high A β ₄₀:42 ratio favors the development of CAA (74, 77). The APPDutch animal model, that recapitulates the characteristics of hereditary cerebral hemorrhage with amyloidosis-Dutch type (HCHWA-D) and shows A β accumulation predominantly in the cerebral vessels, appears to have a highly elevated A β ₄₀:42 ratio when compared to animals overexpressing human wild-type APP (77). In addition, it has been reported that Tg2576 mice expressing human ApoE4, develop CAA which is also likely attributable to the higher ratio of A β ₄₀:42 in these animals in relation to animals expressing endogenous murine ApoE (74). In contrast, a lower A β ₄₀:42 ratio seems to promote amyloid deposition in brain parenchyma versus cerebrovasculature. It has been shown that APP mice harboring the "Indiana" mutation, which leads to the highly elevated levels of A β ₄₂, have a reduction in A β ₄₀:42 ratio and therefore mainly parenchymal deposition of A β (78). This notion is further supported by observation that PDAPP mice lacking ApoE have an increased production of A β ₄₂, which results in deposition of parenchymal amyloid with very minimal CAA (76).

Among numerous A β clearance pathways in the brain that have previously been described (57, 68, 79-84), perivascular drainage along basement membranes of cerebral arteries is one of the major routes for A β removal and its impairment leads to CAA formation (25, 26). We found a reduced number of arteries with co-localization of injected fluorescent A β in the basement membranes in *Clu*^{-/-} mice compared to control littermates, suggesting the disruption of perivascular drainage of A β in the absence of CLU. Consistent with this notion, we found direct *ex vivo* evidence that CLU alters A β binding to isolated cerebral vessels, which might exacerbate development of CAA. Therefore we propose that CLU facilitates A β clearance along ISF drainage pathways by preventing binding to cerebral vessels possibly through the interactions with cerebrovascular basement membrane components. Thus, as a consequence of CLU loss, A β fibrils accumulate in the cerebral vessels and lead to CAA.

Interestingly, using unbiased proteomic analysis, we have recently demonstrated that the level of CLU protein is significantly elevated in human leptomeningeal arteries with CAA (85), suggesting the entrapment of the A β -CLU complex in the perivascular drainage pathways, or a compensatory up-regulation of CLU to clear A β .

Despite the evidence that loss of CLU leads to the accumulation of A β in the walls of cerebral vessels, possibly mediating the formation of CAA, we cannot rule out the possibility that other mechanisms also contribute to A β deposition in different brain compartments. Previous reports have demonstrated that the transport of soluble A β across the blood brain barrier (BBB) can be facilitated via low-density lipoprotein receptor-related protein-1 (LRP1) (84). In addition, the low density lipoprotein receptor-related protein-2 (LRP2) has been previously shown to mediate the elimination of A β ₄₂ from the brain. LRP2 is a

receptor for CLU localized at the BBB and it has been suggested to be essential for the transport of the A β -CLU complex into circulation (57). It is possible, that the absence of CLU also disrupts the A β transport across BBB via LRP2, leading to the accumulation of A β within the walls of the cerebrovasculature. Although the BBB plays a significant role in the A β clearance, whether and to what extend BBB transporters contribute to the development of CAA in APP/PS1; *Clu*^{-/-} mice is yet to be determined, although we found no evidence of altered transcript levels of *Lrp1*, *Lrp2*, or other members of the LDLR family in our RNAseq data.

Mounting evidence has demonstrated the strong association between CAA and cerebral hemorrhage in elderly individuals. Recurrent cerebral hemorrhage is also present in patients with hereditary cerebral hemorrhage with amyloidosis Icelandic type (HCHWA-I), however it is also frequently observed in individuals with sporadic CAA (86, 87). Several lines of evidence suggest that cerebral hemorrhage is caused by gradual smooth muscle cell degeneration in the walls of cerebral vessels leading to their weakening and rupture (88). Spontaneous acute hemorrhage has also been linked to widespread A β deposition in leptomeningeal and cortical vessels in several transgenic mice. Winkler et al. showed that accumulation of A β is sufficient to give rise to recurrent hemorrhagic stroke in APP23 mice (89). Similar findings have been reported for other transgenic mouse models overexpressing human APP harboring various mutations including Tg2576, PDAPP (76), TgSwDI (90), and APPDutch (77) that develop spontaneous hemorrhage in association with A β -laden vessels. Interestingly, the loss of ApoE in Tg2576 and PDAPP mice completely prevented CAA and hemorrhage, indicating that ApoE facilitates CAA and CAA-associated hemorrhage (76). Although CAA is a major risk factor for developing hemorrhage, we observed a significant decrease in the number of microhemorrhages in APP/PS1; *Clu*^{-/-} mice compared to APP/PS1; *Clu*^{+/+} animals. A possible explanation for this difference with previous studies could be that CLU expression alters the structure and/or amount of amyloid deposited in the walls of cerebrovasculature causing their damage.

It is recognized that neuroinflammation is another component commonly observed in individuals with CAA (91). Similar to human studies, Herzig et al. have observed that an inflammatory response is associated with vascular amyloid and exists independently from amyloid plaques in APPDutch mice (77). Miao et al. have shown that reactive astrocytes and activated microglia were present in vicinity of A β -laden vessels in Tg-SwDI transgenic mice (92). In addition, elevated levels of inflammatory cytokines including IL-6 and IL-1 β were noted in these animals (92). While these studies support an association of vascular amyloid with neuroinflammation, the majority of CAA in these models is weighted toward capillaries. Our data indicate that the cellular and molecular inflammation are more associated with parenchymal amyloid load rather than CAA. These observations raise the possibility that CAA as seen in sporadic CAA is not sufficient to cause neuroinflammation in APP/PS1 mice or that the combination of CAA and CLU expression is critical for induction of inflammatory response. Additional studies are needed to further address this issue.

Given the role of CLU in A β accumulation, transport, and toxicity, and its strong genetic association with AD, we aimed to elucidate how CLU affects A β pathology and discovered a novel role in the pathophysiology of both parenchymal plaque formation as well as CAA. Future studies are crucial to gain a detailed view of additional mechanisms underlying the role of CLU in CAA and to better understand specific events leading to pathogenesis of AD and CAA. This could allow optimization of therapeutic strategies to limit A β deposition in brain parenchyma and cerebrovasculature. Therapeutics that intentionally or unin-

1089 tententionally decrease the levels of CLU may result in an unwanted
1090 shift of Aβ pathology to CAA, although our data indicate that the
1091 brain may be more tolerant of amyloid in the cerebrovasculature
1092 than in the parenchyma.

1093 Materials and Methods

1094 Animals

1095 APP/PS1 mice bearing a double mutation APPswe/PS1ΔE9 were used
1096 (65). All studies were done in accordance with National Institutes of Health
1097 Guide for the Care and Use of Laboratory Animals under an approved
1098 protocol from the Mayo Clinic Institutional Animal Care and Use Committee.
1099 De-identified post-mortem, pathologically confirmed Alzheimer's disease
1100 brain tissue was obtained through the Mayo Clinic Brain Bank for neurode-
1101 generative diseases, whose operating procedures are approved by the Mayo
1102 Institutional Review Board.

1103 Histopathological analyses

1104 PBS perfused brains from APP/PS1; *Clu*^{+/-} and APP/PS1; *Clu*^{-/-} mice were
1105 used and analyzed using a Zeiss AxioImager.Z1/ApoTome microscope. Aβ
1106 pathology was quantified, as previously described(76).

1107 Biochemical analyses

1108 Cortex and hippocampus were dissected from APP/PS1; *Clu*^{+/-} and
1109 APP/PS1; *Clu*^{-/-} PBS perfused brains. Separate extraction for each condition
1110 was used. Aβ₄₀ and Aβ₄₂ levels were assessed by ELISAs. To examine APP
1111 processing, cortex of APP/PS1; *Clu*^{+/-} and APP/PS1; *Clu*^{-/-} mice was used. Total

- 1112 1. Anonymous (2014) 2014 Alzheimer's disease facts and figures. *Alzheimer's & dementia : the*
1113 *journal of the Alzheimer's Association* 10(2):e47-92.
- 1114 2. Vassar R, *et al.* (1999) Beta-secretase cleavage of Alzheimer's amyloid precursor protein by
1115 the transmembrane aspartic protease BACE. *Science* 286(5440):735-741.
- 1116 3. Kimberly WT, *et al.* (2003) Gamma-secretase is a membrane protein complex comprised of
1117 presenilin, nicastrin, Aph-1, and Pen-2. *Proc Natl Acad Sci U S A* 100(11):6382-6387.
- 1118 4. Glenner GG & Wong CW (1984) Alzheimer's disease: initial report of the purification and
1119 characterization of a novel cerebrovascular amyloid protein. *Biochemical and biophysical*
1120 *research communications* 120(3):885-890.
- 1121 5. Grundke-Iqbal I, *et al.* (1986) Microtubule-associated protein tau. A component of
1122 Alzheimer paired helical filaments. *J Biol Chem* 261(13):6084-6089.
- 1123 6. Walsh DM & Selkoe DJ (2004) Deciphering the molecular basis of memory failure in
1124 Alzheimer's disease. *Neuron* 44(1):181-193.
- 1125 7. Vinters HV (1987) Cerebral amyloid angiopathy. A critical review. *Stroke; a journal of cerebral*
1126 *circulation* 18(2):311-324.
- 1127 8. Jellinger KA (2002) Alzheimer disease and cerebrovascular pathology: an update. *Journal of*
1128 *neurotransmission* 109(5-6):813-836.
- 1129 9. Roher AE, *et al.* (2003) Cortical and leptomeningeal cerebrovascular amyloid and white
1130 matter pathology in Alzheimer's disease. *Molecular medicine* 9(3-4):112-122.
- 1131 10. Revesz T, *et al.* (2002) Sporadic and familial cerebral amyloid angiopathies. *Brain pathology*
1132 12(3):343-357.
- 1133 11. Yamada M (2015) Cerebral amyloid angiopathy: emerging concepts. *Journal of stroke*
1134 17(1):17-30.
- 1135 12. Levy E, *et al.* (1990) Mutation of the Alzheimer's disease amyloid gene in hereditary cerebral
1136 hemorrhage, Dutch type. *Science* 248(4959):1124-1126.
- 1137 13. Maat-Schieman M, Roos R, & van Duinen S (2005) Hereditary cerebral hemorrhage
1138 with amyloidosis-Dutch type. *Neuropathology : official journal of the Japanese Society of*
1139 *Neuropathology* 25(4):288-297.
- 1140 14. Grabowski TJ, Cho HS, Vonsattel JP, Rebeck GW, & Greenberg SM (2001) Novel amyloid
1141 precursor protein mutation in an Iowa family with dementia and severe cerebral amyloid
1142 angiopathy. *Annals of neurology* 49(6):697-705.
- 1143 15. Bugiani O, *et al.* (2010) Hereditary cerebral hemorrhage with amyloidosis associated with the
1144 E693K mutation of APP. *Archives of neurology* 67(8):987-995.
- 1145 16. Goate A, *et al.* (1991) Segregation of a missense mutation in the amyloid precursor protein
1146 gene with familial Alzheimer's disease. *Nature* 349(6311):704-706.
- 1147 17. Mullan M, *et al.* (1992) A pathogenic mutation for probable Alzheimer's disease in the APP
1148 gene at the N-terminus of beta-amyloid. *Nature genetics* 1(5):345-347.
- 1149 18. Van Broeckhoven C, *et al.* (1992) Mapping of a gene predisposing to early-onset Alzheimer's
1150 disease to chromosome 14q24.3. *Nature genetics* 2(4):335-339.
- 1151 19. Cruts M, *et al.* (1998) Estimation of the genetic contribution of presenilin-1 and -2 mutations
1152 in a population-based study of presenile Alzheimer disease. *Human molecular genetics*
1153 7(1):43-51.
- 1154 20. Levy-Lahad E, *et al.* (1995) A familial Alzheimer's disease locus on chromosome 1. *Science*
1155 269(5226):970-973.
- 1156 21. Borchelt DR, *et al.* (1996) Familial Alzheimer's disease-linked presenilin 1 variants elevate
Aβ₄₂/Aβ₄₀ ratio in vitro and in vivo. *Neuron* 17(5):1005-1013.
22. Xia W, *et al.* (1997) Enhanced production and oligomerization of the 42-residue amyloid
beta-protein by Chinese hamster ovary cells stably expressing mutant presenilins. *J Biol Chem*
272(12):7977-7982.
23. Tarasoff-Conway JM, *et al.* (2015) Clearance systems in the brain-implications for Alzheimer
disease. *Nature reviews. Neurology* 11(8):457-470.
24. Weller RO, Subash M, Preston SD, Mazanti I, & Carare RO (2008) Perivascular drainage
of amyloid-beta peptides from the brain and its failure in cerebral amyloid angiopathy and
Alzheimer's disease. *Brain pathology* 18(2):253-266.
25. Hawkes CA, *et al.* (2011) Perivascular drainage of solutes is impaired in the ageing mouse
brain and in the presence of cerebral amyloid angiopathy. *Acta neuropathologica* 121(4):431-

RNA was isolated using a Total Aurum RNA isolation kit. Random-primed
reverse transcription was performed. All samples were run on an ABI 7900
HT Fast Real Time PCR instrument.

1159 In vivo clearance

1160 In vivo microdialysis in APP/PS1; *Clu*^{+/-} and APP/PS1; *Clu*^{-/-} mice was
1161 performed, as described (69, 94). Perivascular drainage was quantified in
1162 *Clu*^{+/-} and *Clu*^{-/-} mice, as described (25).

1163 Aβ binding to cerebrovasculature

1164 Cerebral vessels were isolated from C57Bl/6J mice, as described (76).
1165 Vessels were treated with Aβ₄₀ or Aβ₄₂ with or without CLU. The Aβ binding
1166 to vasculature was assessed by ELISA.

1167 Statistical analyses

1168 For all statistical analyses GraphPad Prism 5.04 software was used.
1169 For additional descriptions of methods, please see *SI Materials and*
1170 *Methods*.

1171 Acknowledgements

1172 Funding sources for JDF: Mayo Foundation, GHR Foundation, Mayo
1173 Clinic Center for Individualized Medicine, Mayo Clinic Gerstner Family Career
1174 Development Award, Ed and Ethel Moore Alzheimer's Disease Research
1175 Program of Florida Department of Health (6A206), and NIH N5094137,
1176 AG047327, and AG049992. Funding sources for SK: The Robert and Clarice
1177 Smith and Abigail Van Buren Alzheimer's Disease Research Program Fel-
1178 lowship, Mayo Clinic Program on Synaptic Biology and Memory, and
1179 NIH MH103632. Funding sources for GB: NIH AG027924, AG035355, and
1180 NS074969.

- 1181 443.
- 1182 26. Hawkes CA, *et al.* (2012) Disruption of arterial perivascular drainage of amyloid-beta from
1183 the brains of mice expressing the human APOE epsilon4 allele. *PLoS one* 7(7):e41636.
- 1184 27. Hawkes CA, Gentleman SM, Nicoll JA, & Carare RO (2015) Prenatal high-fat diet alters the
1185 cerebrovasculature and clearance of beta-amyloid in adult offspring. *J Pathol* 235(4):619-631.
- 1186 28. Jenne DE, *et al.* (1991) Clusterin (complement lysis inhibitor) forms a high density lipoprotein
1187 complex with apolipoprotein A-I in human plasma. *J Biol Chem* 266(17):11030-11036.
- 1188 29. de Silva HV, Harmony JA, Stuart WD, Gil CM, & Robbins J (1990) Apolipoprotein J:
1189 structure and tissue distribution. *Biochemistry* 29(22):5380-5389.
- 1190 30. de Silva HV, *et al.* (1990) A 70-kDa apolipoprotein designated ApoJ is a marker for subclasses
1191 of human plasma high density lipoproteins. *J Biol Chem* 265(22):13240-13247.
- 1192 31. Jenne DE & Tschopp J (1992) Clusterin: the intriguing guises of a widely expressed glyco-
1193 protein. *Trends Biochem Sci* 17(4):154-159.
- 1194 32. Hermo L, Barin K, & Oko R (1994) Developmental expression of sulfated glycoprotein-2 in
1195 the epididymis of the rat. *Anat Rec* 240(3):327-344.
- 1196 33. Silksens JR, *et al.* (1995) Clusterin promotes the aggregation and adhesion of renal porcine
1197 epithelial cells. *J Clin Invest* 96(6):2646-2653.
- 1198 34. Purrello M, *et al.* (1991) The gene for SP-40,40, human homolog of rat sulfated glycoprotein
1199 2, rat clusterin, and rat testosterone-repressed prostate message 2, maps to chromosome 8.
1200 *Genomics* 10(1):151-156.
- 1201 35. Wong P, *et al.* (1994) Molecular characterization of human TRPM-2/clusterin, a gene asso-
1202 ciated with sperm maturation, apoptosis and neurodegeneration. *Eur J Biochem* 221(3):917-
1203 925.
- 1204 36. Kirszenbaum L, Bozas SE, & Walker ID (1992) SP-40,40, a protein involved in the control of
1205 the complement pathway, possesses a unique array of disulphide bridges. *FEBS Lett* 297(1-
1206 2):70-76.
- 1207 37. Wilson MR & Easterbrook-Smith SB (2000) Clusterin is a secreted mammalian chaperone.
1208 *Trends Biochem Sci* 25(3):95-98.
- 1209 38. Bartl MM, Luckenbach T, Bergner O, Ullrich O, & Koch-Brandt C (2001) Multiple receptors
1210 mediate apoJ-dependent clearance of cellular debris into nonprofessional phagocytes. *Exp*
1211 *Cell Res* 271(1):130-141.
- 1212 39. Wyatt AR, *et al.* (2011) Clusterin facilitates in vivo clearance of extracellular misfolded
1213 proteins. *Cell Mol Life Sci* 68(23):3919-3931.
- 1214 40. Leskov KS, Klokoy DY, Li J, Kinsella TJ, & Boothman DA (2003) Synthesis and functional
1215 analyses of nuclear clusterin, a cell death protein. *J Biol Chem* 278(13):11590-11600.
- 1216 41. Yang CR, *et al.* (2000) Nuclear clusterin/XIP8, an x-ray-induced Ku70-binding protein that
1217 signals cell death. *Proc Natl Acad Sci U S A* 97(11):5907-5912.
- 1218 42. Aronow BJ, Lund SD, Brown TL, Harmony JA, & Witte DP (1993) Apolipoprotein J
1219 expression at fluid-tissue interfaces: potential role in barrier cytoprotection. *Proc Natl Acad*
1220 *Sci U S A* 90(2):725-729.
- 1221 43. Verbrugge P, Kujala P, Waelput W, Peters PJ, & Cuvelier CA (2008) Clusterin in human
1222 gut-associated lymphoid tissue, tonsils, and adenoids: localization to M cells and follicular
1223 dendritic cells. *Histochem Cell Biol* 129(3):311-320.
- 1224 44. Shin JK, *et al.* (2008) Expression of clusterin in normal and preeclamptic placentas. *J Obstet*
Gynaecol Res 34(4):473-479.
45. Danik M, Chabot JG, Hassan-Gonzalez D, Suh M, & Quirion R (1993) Localization of
sulfated glycoprotein-2/clusterin mRNA in the rat brain by in situ hybridization. *J Comp*
Neurol 334(2):209-227.
46. O'Bryan MK, Cheema SS, Bartlett PF, Murphy BE, & Pearse MJ (1993) Clusterin levels
increase during neuronal development. *J Neurobiol* 24(4):421-432.
47. Pasinetti GM, Johnson SA, Oda T, Rozovsky I, & Finch CE (1994) Clusterin (SGP-2): a
multifunctional glycoprotein with regional expression in astrocytes and neurons of the adult
rat brain. *J Comp Neurol* 339(3):387-400.
48. Corder EH, *et al.* (1993) Gene dose of apolipoprotein E type 4 allele and the risk of
Alzheimer's disease in late onset families. *Science* 261(5123):921-923.
49. Greenberg SM, *et al.* (1996) Apolipoprotein E epsilon 4 is associated with the presence and

- earlier onset of hemorrhage in cerebral amyloid angiopathy. *Stroke; a journal of cerebral circulation* 27(8):1333-1337.
50. May PC & Finch CE (1992) Sulfated glycoprotein 2: new relationships of this multifunctional protein to neurodegeneration. *Trends Neurosci* 15(10):391-396.
 51. May PC, *et al.* (1990) Dynamics of gene expression for a hippocampal glycoprotein elevated in Alzheimer's disease and in response to experimental lesions in rat. *Neuron* 5(6):831-839.
 52. Matsubara E, Frangione B, & Ghiso J (1995) Characterization of apolipoprotein J-Alzheimer's A beta interaction. *J Biol Chem* 270(13):7563-7567.
 53. Oda T, *et al.* (1995) Clusterin (apoJ) alters the aggregation of amyloid beta-peptide (A beta 1-42) and forms slowly sedimenting A beta complexes that cause oxidative stress. *Experimental neurology* 136(1):22-31.
 54. Matsubara E, Soto C, Governale S, Frangione B, & Ghiso J (1996) Apolipoprotein J and Alzheimer's amyloid beta solubility. *The Biochemical journal* 316 (Pt 2):671-679.
 55. DeMattos RB, *et al.* (2004) ApoE and clusterin cooperatively suppress Abeta levels and deposition: evidence that ApoE regulates extracellular Abeta metabolism in vivo. *Neuron* 41(2):193-202.
 56. DeMattos RB, *et al.* (2002) Clusterin promotes amyloid plaque formation and is critical for neuritic toxicity in a mouse model of Alzheimer's disease. *Proc Natl Acad Sci U S A* 99(16):10843-10848.
 57. Bell RD, *et al.* (2007) Transport pathways for clearance of human Alzheimer's amyloid beta-peptide and apolipoproteins E and J in the mouse central nervous system. *J Cereb Blood Flow Metab* 27(5):909-918.
 58. Zlokovic BV, *et al.* (1994) Brain uptake of circulating apolipoproteins J and E complexed to Alzheimer's amyloid beta. *Biochemical and biophysical research communications* 205(2):1431-1437.
 59. Zlokovic BV, *et al.* (1996) Glycoprotein 330/megalin: probable role in receptor-mediated transport of apolipoprotein J alone and in a complex with Alzheimer disease amyloid beta at the blood-brain and blood-cerebrospinal fluid barriers. *Proc Natl Acad Sci U S A* 93(9):4229-4234.
 60. Harold D, *et al.* (2009) Genome-wide association study identifies variants at CLU and PICALM associated with Alzheimer's disease. *Nature genetics* 41(10):1088-1093.
 61. Lambert JC, *et al.* (2009) Genome-wide association study identifies variants at CLU and CR1 associated with Alzheimer's disease. *Nature genetics* 41(10):1094-1099.
 62. Carrasquillo MM, *et al.* (2010) Replication of CLU, CR1, and PICALM associations with alzheimer disease. *Archives of neurology* 67(8):961-964.
 63. Corneveaux JJ, *et al.* (2010) Association of CR1, CLU and PICALM with Alzheimer's disease in a cohort of clinically characterized and neuropathologically verified individuals. *Human molecular genetics* 19(16):3295-3301.
 64. Bettens K, *et al.* (2012) Both common variations and rare non-synonymous substitutions and small insertion/deletions in CLU are associated with increased Alzheimer risk. *Molecular neurodegeneration* 7:3.
 65. Jankowsky JL, *et al.* (2004) Mutant presenilins specifically elevate the levels of the 42 residue beta-amyloid peptide in vivo: evidence for augmentation of a 42-specific gamma secretase. *Human molecular genetics* 13(2):159-170.
 66. Weekman EM, *et al.* (2016) Reduced Efficacy of Anti-Abeta Immunotherapy in a Mouse Model of Amyloid Deposition and Vascular Cognitive Impairment Comorbidity. *J Neurosci* 36(38):9896-9907.
 67. Kinnecom C, *et al.* (2007) Course of cerebral amyloid angiopathy-related inflammation. *Neurology* 68(17):1411-1416.
 68. Wyss-Coray T, *et al.* (2001) TGF-beta1 promotes microglial amyloid-beta clearance and reduces plaque burden in transgenic mice. *Nat Med* 7(5):612-618.
 69. Cirrito JR, *et al.* (2003) In vivo assessment of brain interstitial fluid with microdialysis reveals plaque-associated changes in amyloid-beta metabolism and half-life. *The Journal of neuroscience : the official journal of the Society for Neuroscience* 23(26):8844-8853.
 70. Suzuki N, *et al.* (1994) High tissue content of soluble beta 1-40 is linked to cerebral amyloid angiopathy. *Am J Pathol* 145(2):452-460.
 71. Alonzo NC, Hyman BT, Rebeck GW, & Greenberg SM (1998) Progression of cerebral amyloid angiopathy: accumulation of amyloid-beta40 in affected vessels. *J Neuropathol Exp Neurol* 57(4):353-359.
 72. Jarrett JT, Berger EP, & Lansbury PT, Jr. (1993) The carboxy terminus of the beta amyloid protein is critical for the seeding of amyloid formation: implications for the pathogenesis of Alzheimer's disease. *Biochemistry* 32(18):4693-4697.
 73. Walsh DM, Lomakin A, Benedek GB, Condron MM, & Teplow DB (1997) Amyloid beta-protein fibrillogenesis. Detection of a protofibrillar intermediate. *J Biol Chem* 272(35):22364-22372.
 74. Fryer JD, *et al.* (2005) Human apolipoprotein E4 alters the amyloid-beta 40:42 ratio and promotes the formation of cerebral amyloid angiopathy in an amyloid precursor protein transgenic model. *The Journal of neuroscience : the official journal of the Society for Neuroscience* 25(11):2803-2810.
 75. Herzig MC, Van Nostrand WE, & Jucker M (2006) Mechanism of cerebral beta-amyloid angiopathy: murine and cellular models. *Brain pathology* 16(1):40-54.
 76. Fryer JD, *et al.* (2003) Apolipoprotein E markedly facilitates age-dependent cerebral amyloid angiopathy and spontaneous hemorrhage in amyloid precursor protein transgenic mice. *The Journal of neuroscience : the official journal of the Society for Neuroscience* 23(21):7889-7896.
 77. Herzig MC, *et al.* (2004) Abeta is targeted to the vasculature in a mouse model of hereditary cerebral hemorrhage with amyloidosis. *Nature neuroscience* 7(9):954-960.
 78. Hsiao K, *et al.* (1996) Correlative memory deficits, Abeta elevation, and amyloid plaques in transgenic mice. *Science* 274(5284):99-102.
 79. Bu G (2009) Apolipoprotein E and its receptors in Alzheimer's disease: pathways, pathogenesis and therapy. *Nat Rev Neurosci* 10(5):333-344.
 80. Wyss-Coray T, *et al.* (2003) Adult mouse astrocytes degrade amyloid-beta in vitro and in situ. *Nat Med* 9(4):453-457.
 81. El Khoury J & Luster AD (2008) Mechanisms of microglia accumulation in Alzheimer's disease: therapeutic implications. *Trends Pharmacol Sci* 29(12):626-632.
 82. Weller RO, *et al.* (1998) Cerebral amyloid angiopathy: amyloid beta accumulates in putative interstitial fluid drainage pathways in Alzheimer's disease. *Am J Pathol* 153(3):725-733.
 83. Revesz T, *et al.* (2003) Cerebral amyloid angiopathies: a pathologic, biochemical, and genetic view. *J Neuropathol Exp Neurol* 62(9):885-898.
 84. Deane R, *et al.* (2004) LRP/amyloid beta-peptide interaction mediates differential brain efflux of Abeta isoforms. *Neuron* 43(3):333-344.
 85. Manousopoulou A, *et al.* (2016) Systems proteomic analysis reveals that Clusterin and Tissue Inhibitor of Metalloproteinases 3 increase in leptomeningeal arteries affected by cerebral amyloid angiopathy. *Neuropathology and applied neurobiology*.
 86. Vinters HV, *et al.* (1998) Secondary microvascular degeneration in amyloid angiopathy of patients with hereditary cerebral hemorrhage with amyloidosis, Dutch type (HCHWA-D). *Acta neuropathologica* 95(3):235-244.
 87. Wattendorff AR, Frangione B, Luyendijk W, & Bots GT (1995) Hereditary cerebral haemorrhage with amyloidosis, Dutch type (HCHWA-D): clinicopathological studies. *Journal of neurology, neurosurgery, and psychiatry* 58(6):699-705.
 88. Maeda A, *et al.* (1993) Computer-assisted three-dimensional image analysis of cerebral amyloid angiopathy. *Stroke; a journal of cerebral circulation* 24(12):1857-1864.
 89. Winkler DT, *et al.* (2001) Spontaneous hemorrhagic stroke in a mouse model of cerebral amyloid angiopathy. *The Journal of neuroscience : the official journal of the Society for Neuroscience* 21(5):1619-1627.
 90. Davis J, *et al.* (2006) Deficient cerebral clearance of vasculotropic mutant Dutch/Iowa Double A beta in human A betaPP transgenic mice. *Neurobiology of aging* 27(7):946-954.
 91. Eng JA, Frosch MP, Choi K, Rebeck GW, & Greenberg SM (2004) Clinical manifestations of cerebral amyloid angiopathy-related inflammation. *Annals of neurology* 55(2):250-256.
 92. Miao J, *et al.* (2005) Cerebral microvascular amyloid beta protein deposition induces vascular degeneration and neuroinflammation in transgenic mice expressing human vasculotropic mutant amyloid beta precursor protein. *Am J Pathol* 167(2):505-515.
 93. Condello C, Schain A, & Grutzendler J (2011) Multicolor time-stamp reveals the dynamics and toxicity of amyloid deposition. *Scientific reports* 1:19.
 94. Liu CC, *et al.* (2016) Neuronal heparan sulfates promote amyloid pathology by modulating brain amyloid-beta clearance and aggregation in Alzheimer's disease. *Sci Transl Med* 8(332):332ra344.